

## CHAMBER SIMULATION OF FINE PARTICLE PENETRATION INTO HOUSES

R. B. Mosley\* and D. J. Greenwell. U. S. Environmental Protection Agency, National Risk Management Research Laboratory, Research Triangle Park, NC 27711.

### ABSTRACT

Exposure to fine particles of outdoor origin has garnered increased interest of late. A number of recent studies have shown a correlation of negative health effects with increases in outdoor fine particles. Since people spend up to 90% of their time indoors, the relationship between indoor and outdoor fine particles has taken on added significance. This paper describes some results from a study in which the processes of particle removal from infiltrating air by building envelopes are simulated in a chamber. The chamber consists of two compartments, each having a volume of 19 m<sup>3</sup>. Particles with aerodynamic diameters in the range of 0.015 to 5 µm are generated in one compartment and then transported through simulated leakage paths to the other compartment under the action of applied pressure differentials. The simulated leakage paths described in this paper consist of horizontal slits (0.508 mm high, 102 mm deep, and 433 mm wide) between aluminum plates. The penetration factor for each size particle is determined by simultaneously measuring the concentrations in the two compartments as a function of time. The penetration factor is obtained through a mathematical solution of the mass balance equations. The measured values of penetration are compared to predictions of a mathematical model describing deposition by the mechanisms of settling and diffusion. At applied pressures of 2 Pa, only 5% of 0.01 µm particles and 60% of 0.025 µm particles pass through the 0.508 mm high slits. At a pressure of 5 Pa, 30% of 0.01 µm particles and 80% of 0.025 µm particles pass through the slits. At 10 Pa, 54% of 0.01 µm particles and 90% of 0.025 µm particles pass through the slits. At 20 Pa, 72% of 0.01 µm particles and 94% of 0.025 µm particles pass through the slits.

Key words: penetration, fine particles, filtering, deposition

### Introduction

Concern over exposure to fine particles (< 2.5 µm in diameter), particularly in the indoor environment, continues to grow. This concern has resulted in increased interest in understanding the exposure one obtains indoors to fine particles that originate outdoors. The entry mechanisms of particles into buildings are not well understood. The sizes and distribution of openings in building shells are especially unclear. Two recent studies, Thatcher and Layton (1995) and Ozkaynak et al. (1996), have concluded that the penetration factor for particles with diameters smaller than 10 µm is unity. Thatcher and Layton (1995) performed particle penetration measurements in a closed, two-story house in California. The entire house was treated as a well-mixed zone even when analyzing the deposition of particles (1 - 25 µm) resuspended on the first

floor. Measurements were performed only on the first floor. Penetration of outdoor particles was ignored during the particle deposition measurements (an assumption that was, at best, valid only during the very early stage of those measurements). Particle concentrations were interpreted in terms of mass concentration lumped into rather wide size bands. The paper concluded that the penetration factor is approximately unity for all particle sizes up to 25  $\mu\text{m}$ . Ozkaynak et al. (1996) reported on a large "Particle Total Exposure Assessment Methodology (PTEAM)" study performed in Riverside, California. This study reported an average air exchange rate of  $0.97 \text{ h}^{-1}$  and a penetration factor of about unity even for 10  $\mu\text{m}$  diameter particles. This relatively large average value of air exchange rate suggests that many of the houses may have been operated with windows open, a circumstance that is likely to imply a penetration factor near unity. The conclusion that the penetration factor is unity seems to imply that particles enter buildings as easily as the air that carries them. This conclusion is quite troublesome in light of the usual recommendations for at-risk individuals to stay indoors on days of poor air quality or when the ambient particle count is high. The question of whether particles penetrate through the openings in buildings with perfect efficiency plays an important role in understanding the relationship between outdoor particle concentrations and human exposure to those particles, especially for individuals who are largely confined to the indoors. However, since people typically spend the majority of their time indoors, this issue is very important to everyone's exposure. The majority of the published information about particle penetration factors has come from the two studies mentioned above. The PTEAM study was not focused on measuring the penetration factor, but merely tried to statistically tease it out during data analysis. While the Thatcher and Layton study did focus on penetration, it is a study of about 2 weeks in only one house and, consequently, is not definitive. While it seems counterintuitive that all particles, especially the large and very small ones, would readily pass through the small openings in a building shell, little work has been done to better understand the mechanisms by which particles are transported into buildings. Lewis (1995) used controlled experiments with well-defined apertures to demonstrate that penetration of particles with diameters larger than 1  $\mu\text{m}$  is a function of applied pressure and particle size. None of the studies to date, however, address the penetration of submicrometer-sized particles into the indoor environment. Penetration of ambient particles to the indoors has important implications for personal PM exposure.

The objective of the present study is to better understand the mechanisms by which outdoor particles enter the indoor environment. While the study is being conducted at both the laboratory- and full-scale levels, only the laboratory results are discussed in this paper. The laboratory study attempts to perform carefully controlled experiments in airtight chambers so that only particles intentionally injected will be observed in the measurements. In the laboratory, well-defined geometric shapes that are more easily modeled than those of the real world are used to simulate the infiltration routes. This paper will report some results with rectangular slits. The laboratory studies are intended to result in mathematical models that will be validated with well defined entry routes and have the ability to extrapolate to the non-ideal entry routes associated with real construction. The results presented here are an extension of a previous study, Mosley

et al. (2001), which concentrated on the particle size range for which deposition is dominated by gravitational settling. This study emphasizes particles in the size range for which deposition is dominated by diffusion.

### **Chamber Description**

The research chamber is illustrated in schematic form in Figure 1. The chamber consists of two compartments with nearly identical volumes (nominally  $19 \text{ m}^3$  each) separated by a partition containing a  $0.6 \times 1.2 \text{ m}$  window in which a panel of designed openings (capillary tubes, slits, or other orifices) is sealed to provide simulated infiltration entry routes of a building. The walls and ceiling of the compartments are made of gypsum board, while the plywood floors are covered by linoleum. A great deal of effort was expended to reduce the leakiness of each compartment. Each compartment has a leak rate of  $0.1 \text{ h}^{-1}$  when pressured to  $125 \text{ Pa}$ . Each compartment has a ceiling fan that is used to mix the air in the compartment. Since the ceiling fans in the two compartments are not identical in either size or location, the possibility exists that the deposition rate constants will differ when the fans are running. Each compartment is equipped with a high efficiency particle air (HEPA) filter capable of reducing the particle concentration in that compartment to less than  $1000 \text{ particles m}^{-3}$  (detection limit) in about 15 minutes. The air circulation duct is shown on top of the chamber. It contains two in-line fans in series, a HEPA filter, and a laminar flow measurement section. In order to generate the pressure difference that drives the airflow through the simulated entry routes, air is extracted from compartment 2, filtered, and injected into compartment 1. The rectangular slits, simulating leakage paths, are formed by stacking aluminum plates ( $3.175 \text{ mm}$  thick,  $101.6 \text{ mm}$  wide, and  $521.9 \text{ mm}$  long) separated by  $0.508 \text{ mm}$  thick spacers made of shim stock. A spacer  $25.4 \text{ mm}$  wide and  $127 \text{ mm}$  long was placed at each end. Three additional spacers  $12.7 \text{ mm}$  wide were placed at equal distances between the two end spacers. Each slit is then broken into four segments of about equal length. The four segments represent a single slit with a length of  $433 \text{ mm}$ . The plates are stacked in a steel frame with long threaded rods used to uniformly compress the plates against the spacers. While it is very difficult and tedious to measure the variability in the height of the horizontal slits, it is easy to visually observe that the spacing of the plates appears quite uniform. The measurements reported here were performed using 140 such slits. The aluminum plates were purchased with a mill finish (6063 - T5/T52 which corresponds to Federal Specification QQ-A - 200/9d). A Pitot tube using a Shortridge flow meter as a sensor measures the flow rate. This flow measurement system was calibrated against both a Roots meter at high flow rates and a dry gas meter at low flow rates. The calibration curve spans a range from about  $0.001$  to  $0.04 \text{ m}^3 \text{ s}^{-1}$ . The Roots meter had an uncertainty of  $\pm 1.5\%$ , and the maximum combined uncertainty of the calibration curve for the Pitot/Shortridge combination was  $15\%$ .

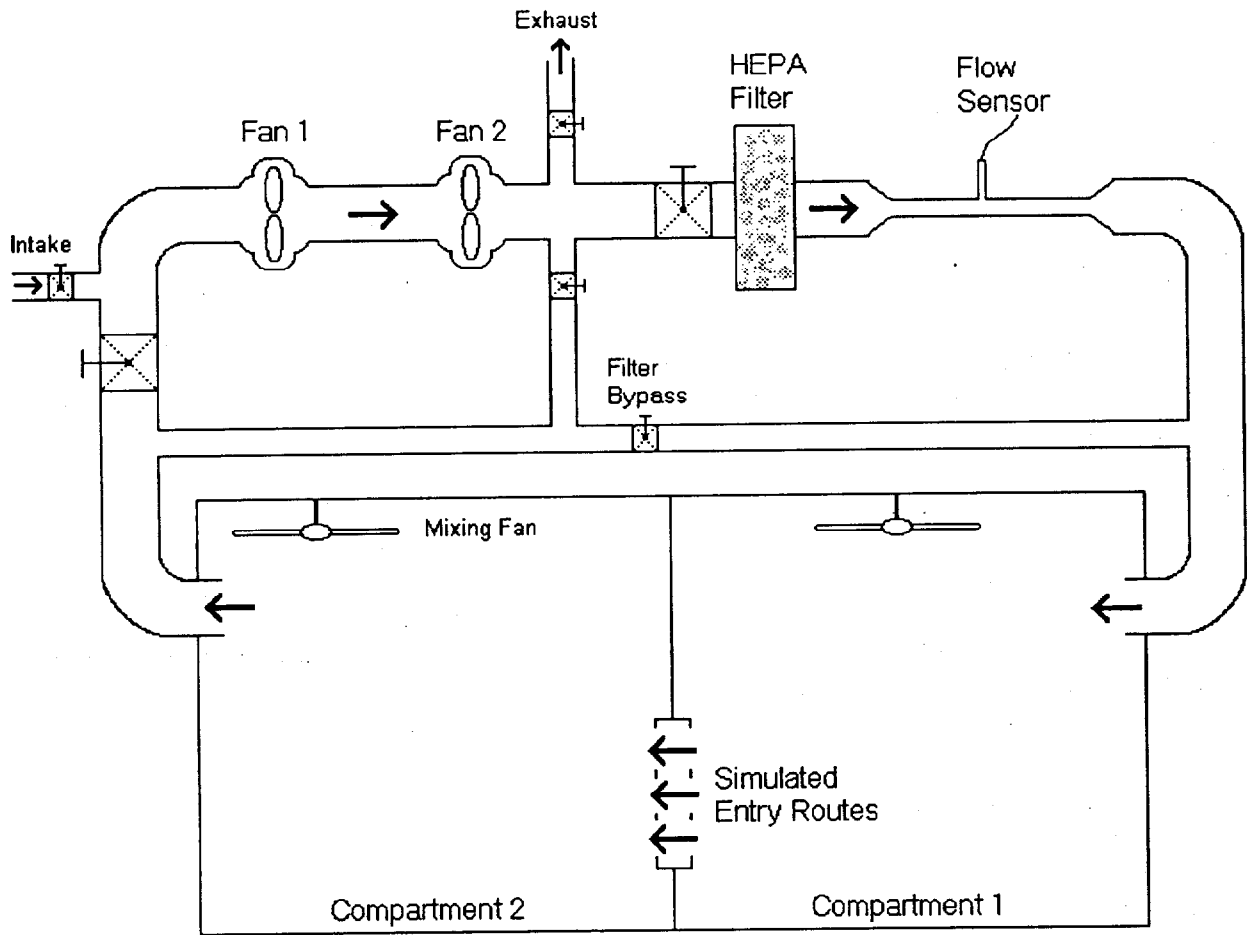


Figure 1. A schematic of the fine particle measurement chamber.

## Experimental Methods

The experiments are intended to simulate entry of particles through building envelopes when all windows and doors are closed. We are studying one well-defined geometric entry route at a time. The present results are for an array of 140 slits 0.508 mm high, 102 mm deep, and 433 mm wide. These open slits constitute an effective leakage area of about 30240 mm<sup>2</sup> or about 0.03 m<sup>2</sup>. Compartment 1 of the chamber simulates the outdoors, while compartment 2 simulates indoor space. The air cleaners are operated to reduce the background concentration in both compartments to below 1000 m<sup>-3</sup> (the detection limit of the instruments). The air cleaner in compartment 1 is turned off and particles are injected, with the mixing fan running, until the desired concentration is obtained. The particle concentration is raised to the optimum range of performance for the measurement instruments. Injection is then stopped and the fan continues running to ensure good mixing in the compartment. The mixing fan continues to operate during the experiment except for studies in quiescent air. When the penetration experiment is ready to start, the air cleaner in compartment 2 is turned off and the circulation fan is turned on at time zero. The circulation fans, used to generate the driving pressure, are controlled by a variac that is manually adjusted to yield the specified pressure. Because of the interactions between the two compartments and the duct with a HEPA filter, it is difficult to maintain a constant pressure between the two compartments. The setting on the variac is tweaked occasionally to maintain a constant pressure. Concentrations in both compartments are then monitored as particles are transported from compartment 1 to compartment 2 by advective flow. Most runs are finished within 2 hours. In most cases, more than one measurement instrument is used to monitor the particle concentration. Timed switching valves allow the same instrument to alternately sample both compartments. As shown in the section on development of equations, the penetration measurement depends, not on the absolute concentration, but on the ratio of the concentrations in the two compartments. For this reason, both concentrations used to compute the ratio are measured with the same instrument. Consequently, the uncertainty in the measured values of penetration due to bias in the instrument will be reduced when the bias is multiplicative. As a result, the importance of the absolute accuracy of the individual concentrations is reduced in the measurement of penetration. The penetration depends on the relative measurements of the two concentrations. Particles were generated from oil (Emery 3004), incense, or sodium chloride (NaCl). The oil and NaCl particles were generated with a condensation monodispersed-aerosol generator.

Data are presented from two particle counters: an electrical low-pressure impactor (ELPI) and a scanning mobility particle sizer (SMPS). The ELPI is an impactor having 12 collection stages with mean particle sizes ranging from 0.04 to 8.5 μm. This instrument provides real-time particle size data, as the measurement is based on the current measured on each stage. The particles pass through a charger and receive a predictable charge before entering the impactor. Electrometers accumulate the charge collected on each stage, and the number of particles contacting each stage is computed. Being an impactor, this size measurement also yields an

aerodynamic diameter. The SMPS uses an electrical classifier to select a very narrow range of particles sizes that are then counted by a condensation nuclei counter. The classifier is automatically scanned through a wide range of voltages covering the entire size range from 0.01 to 1  $\mu\text{m}$  in particle diameter. This size range can be measured in 60 seconds or less. It is sensitive to a range  $10^6 - 10^{13}$  particles  $\text{m}^{-3}$ . The penetration is computed separately for each instrument. The measured penetration involves simultaneous measurements of particle concentrations in each compartment of the chamber, as well as a measurement of the air exchange rate between the compartments.

### Equations Used in the Data Analysis

The principle of mass conservation can be applied to the particles in each compartment to obtain a relationship between the two particle concentrations. A previous study, Mosley et al. (2001), developed the method for analyzing the data to compute the penetration and deposition rate constants. Equations (1) and (2) were derived to describe the concentrations as a function of time in the two compartments:

$$C_1(t) = C_1(0) \exp\left(-\left[\frac{Q}{V} + K_s + K1_d\right]t\right) \quad (1)$$

$$C_2(t) = \exp\left(-\left[\frac{Q}{V} + K_s + K2_d\right]t\right) \left\langle C_2(0) - \frac{PQC_1(0)}{V(K2_d - K1_d)} \{1 - \exp([K2_d - K1_d]t)\} \right\rangle \quad (2)$$

where  $C_1(t)$  is the particle concentration in compartment 1,  $t$  is time,  $C_1(0)$  is the initial concentration in compartment 1,  $Q$  is the volume rate of air flow between compartments,  $V$  is the volume of each compartment,  $K_s$  is the particle decay rate due to gravitational settling,  $K1_d$  is the particle decay rate in compartment 1 due to all other deposition processes (primarily diffusion to the surfaces),  $C_2(t)$  is the particle concentration in compartment 2,  $K2_d$  is the particle decay rate in compartment 2 due to deposition mechanisms other than settling,  $C_2(0)$  is the initial concentration in compartment 2, and  $P$  (the penetration factor) is the fraction of particles leaving compartment 1 by advection that arrive in compartment 2.

In the development, it was shown that, to a good approximation, the ratio of the two concentrations reduces to a simple linear function of time provided the experiment does not last more than an hour or so. That is

$$\frac{C_2(t)}{C_1(t)} = mt \quad (3)$$

where  $m$  is the slope of the resulting linear approximation.

By forming the ratio of the simultaneously measured concentrations in compartments 1 and 2, the ratio becomes a function that is linear with time. The slope,  $m$  (obtained for instance by linear regression), contains the penetration factor,  $P$ . It was shown that the penetration factor is given by:

$$P = \frac{m}{(Q/V)} \quad (4)$$

Note that the quantity  $Q/V$  is the rate of air exchange between the two compartments.

#### **Models for Particle Deposition in Narrow Slits**

Lee and Gieseke (1980) developed Equation (5) to describe the penetration of particles through a parallel plate channel when deposition is dominated by diffusion:

$$P_d = \exp\left(-\frac{1.967DL}{h^2u}\right) \quad (5)$$

where  $P_d$  is the penetration associated with particle diffusion,  $D = (kTC) / (3\pi\mu d)$  is the diffusion coefficient,  $L$  is the depth of the crack,  $2h$  is the height of the crack,  $u = Q/(2hw)$  is the mean flow velocity,  $k$  is Boltzmann's constant,  $T$  is absolute temperature,  $C$  is the Cunningham slip correction factor,  $\mu$  is the viscosity of air,  $d$  is the diameter of the particle, and  $w$  is the length of the crack.

Fuchs (1964) provides Equation (6) for penetration through a crack resulting from gravitational settling:

$$P_g = 1 - \frac{v_s L}{2hu} \quad (6)$$

where  $P_g$  is the penetration factor associated with gravitational settling alone,  $v_s$  is the settling velocity, and  $2h$  is the height of the slit. The other parameters are as previously defined. While inertial deposition was considered in this study, no evidence of this mechanism was observed for the operating conditions studied. Equations (5) and (6) represent individual mechanisms of particle penetration. If the two mechanisms are independent of each other, then the combined effect can be obtained by taking the product:

$$P = P_d P_g \quad (7)$$

Equation (7) represents the model predictions that are compared with penetration measurements in the Results section.

## Results

Figure 2 contains three curves that illustrate how the analysis is carried out. The circles represent the concentration measurements in compartment 1. Note that this concentration decays exponentially with time. The squares represent the particle concentration in compartment 2. It starts at zero and increases with time. Both of these concentrations are read on the axis at the left of the figure. The triangles represent the ratio ( $C_2/C_1$ ) of the two concentrations. This ratio is read from the axis on the right. The solid line is the linear regression fit to the data. The slope [ $m$  in Equation (4)] of the straight line is shown. This value of slope, along with the appropriate value of air exchange rate between compartments 1 and 2, is used to compute the penetration from Equation (7). Similar calculations are performed for each experimental run until a sufficient database of penetrations as a function of particle diameters is obtained.

Measurements of particle penetration through horizontal slits (0.508 mm high, 102 mm deep, and 433 mm wide) are shown in Figures 3 - 6. Data from two different instruments, a scanning mobility particle sizer (SMPS) and an electrical low-pressure impactor (ELPI) are shown. The continuous line shown in all four figures represents a model prediction. The model predictions are from Equation (7). In all four figures, the circles represent averages of SMPS measurements and the squares represent average measurements of the ELPI. The error bars on the individual data symbols correspond to 1 standard deviation from the average.

Figure 3 shows results for an applied pressure of 2 Pa. In Figure 3, the model agrees relatively well with the measurements. Figure 4 shows a similar comparison for the case of 5 Pa applied pressure. Note that slightly more particles of all sizes penetrate the slits than for the 2 Pa case. This results because of the higher flow rate associated with the higher pressure. Higher flow rates correspond to lower residence times for the particles in the slits. Since deposition by both diffusion and settling depend on residence time, fewer particles deposit. This effect is also apparent in Figures 5 and 6. In Figure 5 the applied pressure is 10 Pa, which leads to approximately 70% of the residence time for particles in the slits compared to the 5 Pa case. The value of penetration increases accordingly. In Figure 6 the pressure is doubled again, resulting in a residence time that is about 70% of that in Figure 5. There is a corresponding increase in the penetration for each particle size. Once again the number of particles of a given size that penetrate through the slits increases.

## Discussion

These measurements have attempted to simulate the entry of ambient fine particles into the indoor environment through horizontal slits 0.508 mm high. The applied pressures (2, 5, 10, and 20 Pa) used as driving forces for the entry process are believed to span the realistic range. A negative pressure of 2 Pa in a structure is quite common during much of the year in many regions of moderate climates in the U. S. A negative pressure of 5 Pa in structures is common when the outdoor temperature is near freezing. Outdoor temperatures at and just below freezing will result in negative pressures of 10 Pa in many houses. While a negative pressure of 20 Pa would be rare in moderate climates, it will occur more often in cold climates. A representative set of measurements is shown in Figure 2. The experiment ran for about 1.8 hours. A linear fit to the ratio function appears to be quite good during the entire period of the measurements. However, closer analysis indicates that a slight deviation from linearity begins after about 1 hour. During 1 hour, 30 measurements of concentration are performed in each compartment. This set of measurements was performed for particles with aerodynamic diameters of 1.6  $\mu\text{m}$ . For some larger particles, the deviation from linearity of the ratio function may occur as soon as 30 minutes after the experiment begins. In this case, only 15 pairs of measurements are valid for model analysis. In any event, 15 measurements are probably still adequate for computing an average slope and, thus, particle penetration.

A simple propagation of measurement errors in Equations (3) and (4) provides general bounds on the uncertainty of the measured penetration. The manufacturer specifies an accuracy of  $\pm 10\%$  for particle concentration measurements with the SMPS. As indicated earlier, an uncertainty of  $\pm 15\%$  is associated with the measurement of the flow rate. It follows that the combined uncertainty in the slope computed from Equation (3) would be  $\pm 20\%$  and the combined uncertainty in the penetration from Equation (4) would be  $\pm 35\%$ . The measured penetration of 1.16 (16% greater than the maximum allowed value) at 0.205  $\mu\text{m}$  in Figure 6 is still within the 35% estimated maximum uncertainty.

Another potential source of error relates to the assumption that the gas volumes in the two compartments are well mixed. While definitive measurements to establish a characteristic mixing time have not been performed, some qualitative observations were made. With the mixing fan in compartment 1 running on low speed, the injection was suddenly stopped and the time required for the measured concentration to stop increasing (the sampling port was across the compartment from the injection port) was observed. In this case, measurements were performed every 30 seconds and generally the concentration stopped increasing within 10 minutes. For particles with aerodynamic diameters of 5  $\mu\text{m}$ , the concentration began to decrease almost immediately after turning the injection off. At the beginning of each experiment, particles in compartment 1 were allowed to mix (with the fan on low) for 15 to 45 minutes or longer (depending on the particle size) after turning the injection off and before starting the experiment. Consequently, compartment 1 was always well mixed. Since measurements in compartment 2 were taken every 3 minutes during normal runs, with the entry process continuous, the volume may not have been fully mixed. The error due to lack of complete mixing was probably relatively minor after several measurement cycles. However, the first few measurements probably have substantial error due to incomplete mixing. The total impact of this experimental error on the computed slope of the linear curve is reduced by the fact that the curve is forced to pass through the origin. Consequently, the initial measurements in compartment 2 are less important than the later ones in determining the slope and, thus, the penetration.

A previous study, Mosley et al. (2001), emphasized the large particle limit of these curves where the deposition is dominated by gravitational settling. The experimental data presented in that paper were concentrated at the large particle end of the curves and confirmed the cutoffs suggested by the model predictions. In that study, it was concluded that only 2% of 2  $\mu\text{m}$  particles and 0.1% of 5  $\mu\text{m}$  particles pass through the slits when a pressure of 2 Pa is applied. At a pressure of 5 Pa, 40% of 2  $\mu\text{m}$  particles and less than 1% of 5  $\mu\text{m}$  particles pass through the slits. At 10 Pa, 85% of 2  $\mu\text{m}$  particles and 1% of 5  $\mu\text{m}$  particles pass through the slits. At 20 Pa, 90% of 2  $\mu\text{m}$  particles and 9% of 5  $\mu\text{m}$  particles pass through the slits. The present study emphasizes the small particle end of the curves where deposition is dominated by diffusion.

## **Conclusions**

Particle penetration through narrow (0.508 mm high, 102 mm deep, and 433 mm wide) horizontal slits is a strong function of particle size for applied pressure ranges that are typical of indoor/outdoor pressure differences (2 - 20 Pa). At an applied pressure of 2 Pa, only 5% of 0.01  $\mu\text{m}$  particles and 60% of 0.025  $\mu\text{m}$  particles pass through the 0.508 mm high slits. At a pressure of 5 Pa, 30% of 0.01  $\mu\text{m}$  particles and 80% of 0.025  $\mu\text{m}$  particles pass through the slits. At 10 Pa, 54% of 0.01  $\mu\text{m}$  particles and 90% of 0.025  $\mu\text{m}$  particles pass through the slits. At 20 Pa, 72% of 0.01  $\mu\text{m}$  particles and 94% of 0.025  $\mu\text{m}$  particles pass through the slits.

## References

- Fuchs, C.N., (1964). *The Mechanics of Aerosols*. Pergamon Press, New York, NY.
- Lee, K.W., and Gieseke, J.A., (1980). Simplified Calculation of Aerosol Penetration Through Channels and Tubes. *Atm. Env.*, 14:1089-1094.
- Lewis, S., (1995). Solid Particle Penetration into Enclosures. *J. Haz. Mat.*, 43:195-216.
- Mosley, R.B., Greenwell, D.J., Sparks, L.E., Guo, Z., Tucker, W.G., Fortmann, R., and Whitfield, C., (2001). Penetration of Ambient Particles into the Indoor Environment. *Aerosol Sci. Tech.* 34:127-136.
- Ozkaynak, H., Xue, J., Spengler, J.D., Wallace, L.A., Pellizzari, E.D., and Jenkins, P., (1996). Personal Exposure to Airborne Particles and Metals : Results from a Particle TEAM Study in Riverside, CA. *J. Expos. Anal. and Environ. Epidem.* 6(1):57-78.
- Thatcher, T.L., and Layton, D.W., (1995). Deposition, Resuspension, and Penetration of Particles Within a Residence. *Atm. Env.*, 29:1487-1497.

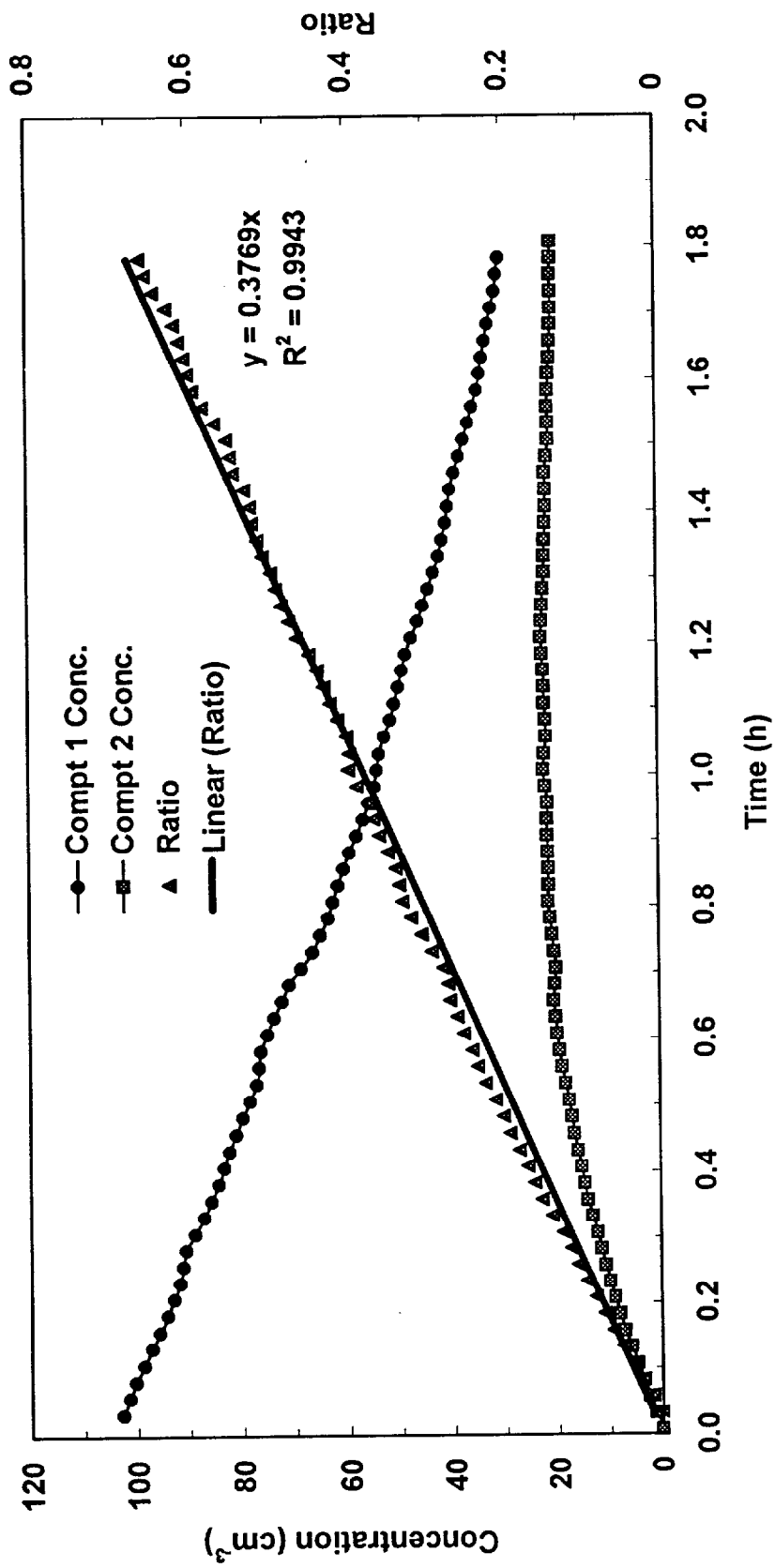


Figure 2. A typical set of concentration measurements in both compartments of the chamber for an Emery oil particle with aerodynamic diameter of 1.6  $\mu\text{m}$ . The ratio of concentrations is also shown to illustrate the method of computing penetration under an applied pressure of 5 Pa.

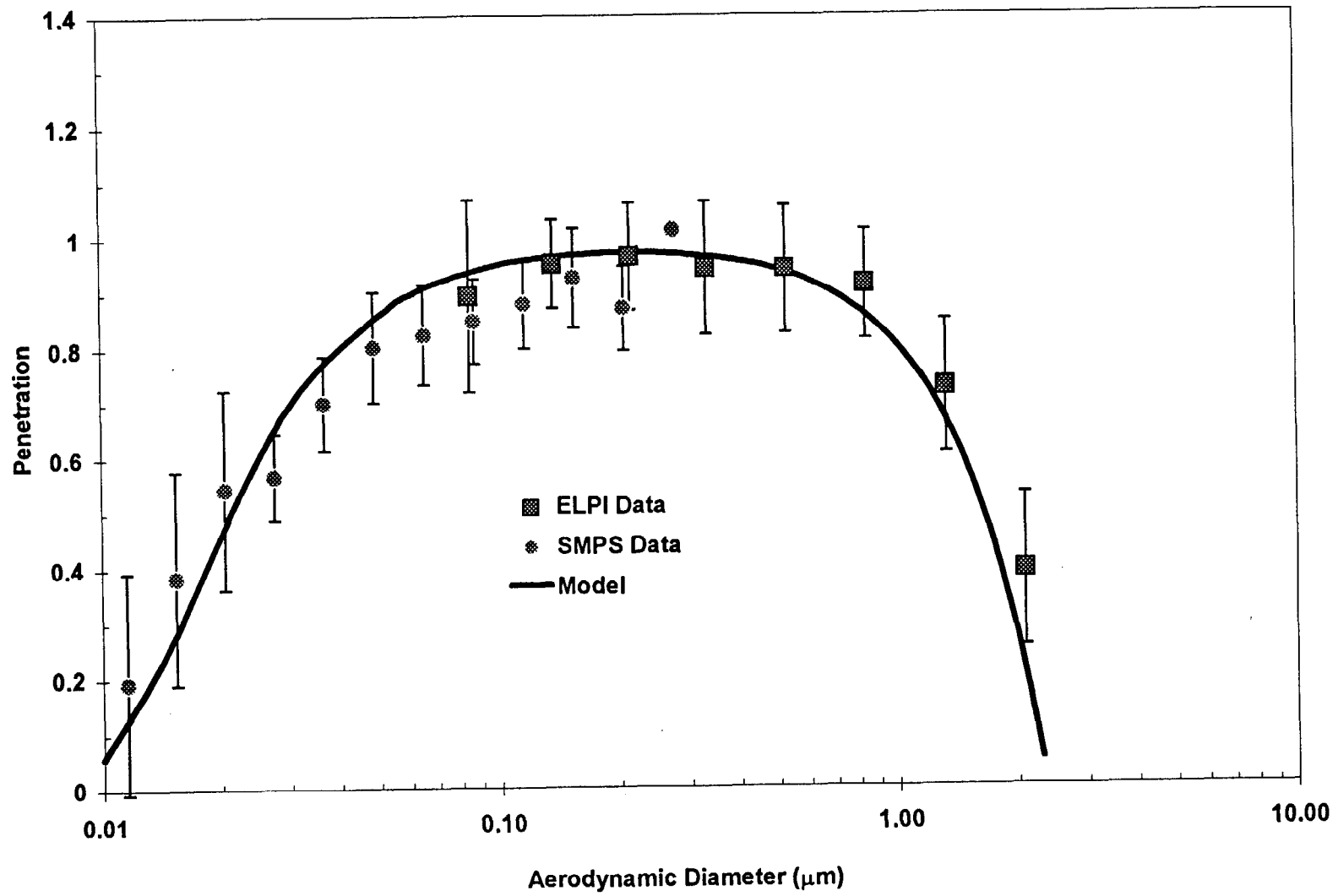


Figure 3. Comparison of penetration measurements and model predictions for 2 Pa pressure applied across 0.5 x 102 mm horizontal slits.

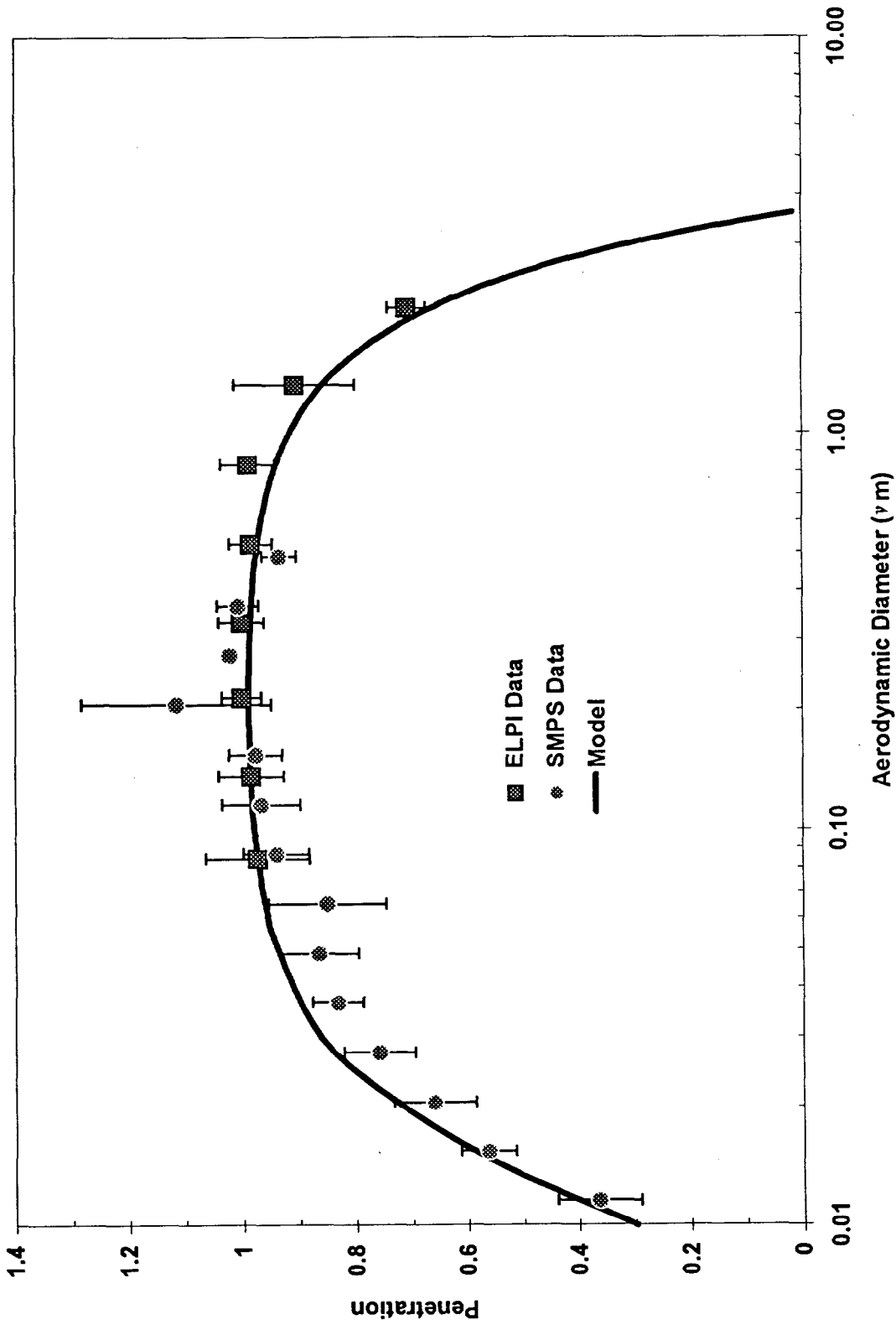


Figure 4. Comparison of penetration measurements and model predictions for 5 Pa pressure applied across 0.5 x 102 mm horizontal slits.

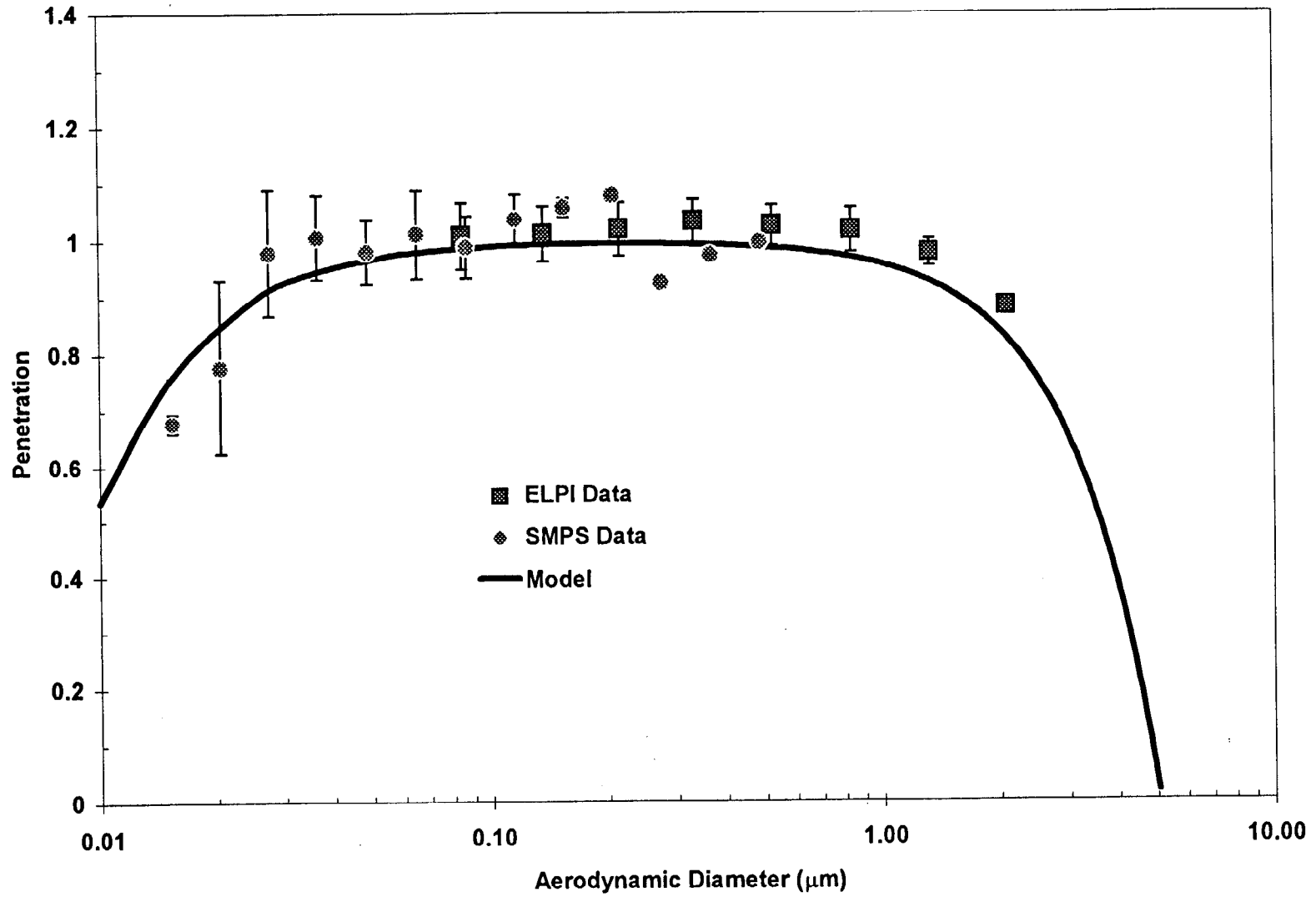


Figure 5. Comparison of penetration measurements and model predictions for 10 Pa pressure applied across 0.5 x 102 mm horizontal slits.

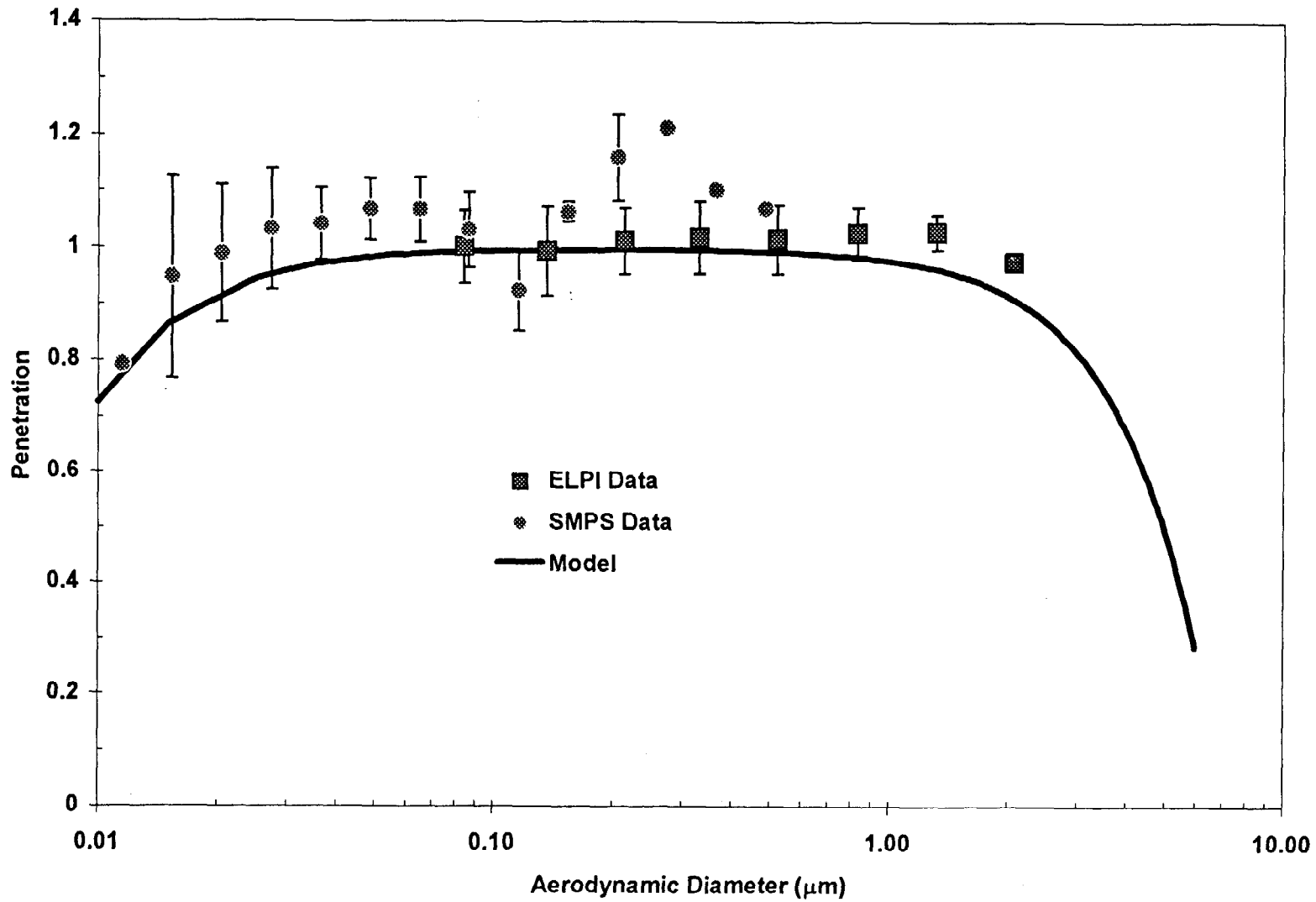


Figure 6. Comparison of penetration measurements and model predictions for 20 Pa pressure applied across 0.5 x 102 mm horizontal slits.